

Comparison of 3D Motion Models for Target Tracking using Quantized Measurements

Fahad A.M, G Sampath Kumar, Dr. Viji Paul P, L Ramakrishnan

Central Research Laboratory, Bharat Electronics Ltd., Jalahalli Post, Bangalore-560013,India.

E-mail : fahad@bel.co.in vijipaulp@bel.co.in

Abstract:

The objective of this paper is to study the performance of interacting multiple model (IMM) filter with constant acceleration (CA), Horizontal constant turn model(HCT) (2D constant turn model with a decoupled filter for height modelled as constant velocity (CV)), 3D constant turn (CT) models and Singer acceleration modes. The existing models will perform effectively for 2D turns. This paper provides a comparative performance analysis of the estimation algorithm with various motion models for 3D turns. Positional error curves have been drawn to show the performance of IMM with 3DCT model and singer models during 3D turns and 2D turns. Monte Carlo simulations shows the capability of singer models to cater wide varieties of 3D target motion.

Key words: maneuvering index, target tracking

I. INTRODUCTION

Tracking a target in space amounts to extracting information of its motion from the available measurements. Most of the algorithms rely on motion models to accomplish this task. Hence the accuracy of motion models in modeling target dynamics gain a significant importance in the realm of target tracking.

Motion models can be classified into two categories: Uniform motion models (straight line motion) and Maneuver motion models. Constant velocity (CV) model, Constant Acceleration (CA) model falls under the former one, whereas the coordinate uncoupled models, coordinate coupled turn models belong to the later. Manoeuvre modeling, which is tedious as compared to uniform motion modelling, had been under limelight over the years. A detailed survey of possible manoeuvre models is described in [1] bringing out their pros and cons. Singer a correlated in time. ‘Current model’ [3] acceleration model [2] laid the foundation for manoeuvre models, wherein the manoeuvres are modelled by acceleration as a random variable effectively a Singer model with adaptive mean for acceleration tries to model manoeuvres. Motion models based on target kinematics are more appealing as the target manoeuvres are usually a turn motion. Such models are coordinate coupled models. Kinematic models to track turns in horizontal plane are derived from curvilinear motion dynamics.

A ‘2D Constant turn (CT) model usually referred to ‘Coordinate Turn’ model is one such type which assumes that turn rate ω is known. A practical approach to track targets in ATC applications is described in [4] which uses multiple turn models with different fixed turn rates.

Augmenting turn rate as a state parameter can give a better estimate but it introduce nonlinearity in state transition. This approach is used in [5] with polar velocity in place of Cartesian velocity.

2D turn models along with height modelled as random walk or constant velocity is suited for ATC applications where the turns are usually in horizontal plane. Tracking military targets capable of performing ‘high g turns ‘in 3D requires coupled models in 3D. 3D Constant Turn (3DCT) model with a known turn rate is described in [6, 7] which assumes that angular velocity is orthogonal to linear velocity making it a ‘3D planar turn model’ (maneuver plane is the plane defined by velocity and acceleration). A 3D constant turn model for unknown turn rate is derived in [8] with angular velocity defined as $\Omega = [\omega_x, \omega_y, \omega_z]$ and is augmented into the state vector. A 3D coordinated turn model is described in [9] for aircrafts with mean thrust(T), mean roll angle(ψ), angle of attack, mean Lift(L).

A target under surveillance can’t be modelled by a single motion model at all instants of time. Therefore, multiple models along with a switching mechanism has to be utilized in reality. Interactive Multiple Model (IMM) is widely accepted in this regime due to its performance in estimating target motion parameters with good accuracy. IMM was first introduced in [10], in which a set of models , with one model active at a time,interact with each other to determine the state of a target. IMM is widely used in tracking with CV,CA,Singer, and CT as its component models. IMM algorithm in [11] compares a combination of CV-3DCT with kinematic constraint with CV-Constant turn Rate filter. IMM using CV,CA,Singer models [12] is tested for targets performing ‘high g-turn’ in 3D space.

We compare Singer acceleration models with different manoeuvre time constants(τ_m) with an IMM filter comprising of CA, Horizontal constant turn model(HCT) (2D constant turn model with a decoupled filter for height modelled as CV) and 3DCT models. Section 2 discuss the motion models specifically Singer Acceleration model, HCT and 3DCT.Section 3 describes IMM Algorithm.Section 4 portraits the Simulation and the performance results.

II. MOTION MODELS IN 3D

Target dynamics and the measurement observation can be mathematically modelled as a continuous state space representation

$$\dot{x}(t) = f(x(t), u(t), t) + w(t) \quad (1)$$

$$z(t) = h(x(t), t) + v(t) \quad (2)$$

Wherein $f(x(t), u(t), t)$ and $h(x(t), t)$ are time varying functions for state propagation and measurement generation respectively. $w(t)$ and $v(t)$ are process noise sequence and measurement noise sequence respectively. $x(t)$, $z(t)$ and $u(t)$ are target state, measurement set and the control input the drives the change in state of the target. Sensors observe the target at discrete intervals of time, t_k , henceforth discrete state space models are preferred in target tracking. Discrete state space models are obtained by discretizing the above continuous state model representations.

$$x_{t+1} = F_t x_t + G_t w_t \quad (3)$$

$$z_t = H_t x_t + v_t \quad (4)$$

Where x_{t+1} and x_t are target states at time t_0 and t_{+1} respectively. F_k and H_k are state transition function and measurement function respectively which can be linear or non linear functions.

Different state models are described with a state vector $x_t = [x, \dot{x}, \ddot{x}, y, \dot{y}, \ddot{y}, z, \dot{z}, \ddot{z}]^T$

Singer acceleration model :

Singer model[2] models target manoeuvre by acceleration correlated in time. It assumes that the acceleration $a(t)$ is zero mean first order stationary Markov process with autocorrelation function defined as $R_a(\tau) = \sigma^2 e^{-\alpha|\tau|}$, where in σ^2 is the variance of acceleration and α , the reciprocal of manoeuvre time, $\alpha = 1/\tau_m$.

The state process of such a linear time invariant system is

$$\dot{a}(t) = -\alpha a(t) + w(t) \quad (5)$$

Where $w(t)$ is a noise sequence with constant power spectral density $S_w = 2\alpha\sigma^2$. Its discrete equivalent is

$$a_{t+1} = e^{-\alpha T} a_t + w_t^a \quad (6)$$

Where w_t^a is zero mean white noise sequence with a variance $\sigma^2(1 - e^{-2\alpha T})$.

The continuous state space representation of Singer model is

$$\dot{x}(t) = \begin{bmatrix} 0 & 1 & 0 \\ 0 & 0 & 1 \\ 0 & 0 & -\alpha \end{bmatrix} x(t) + \begin{bmatrix} 0 \\ 0 \\ 1 \end{bmatrix} w(t) \quad (7)$$

Its discrete equivalent model is

$$x_{t+1} = F_t x_t + w_t \quad (8)$$

Where w_k is zero mean noise sequence whose exact covariance is defined in [2]

and $F_t = \text{diag}(F_\alpha, F_\alpha, F_\alpha)$

$$F_\alpha = \begin{bmatrix} 1 & T & (\alpha T - 1 + e^{-\alpha T})/\alpha^2 \\ 0 & 1 & (1 - e^{-\alpha T})/\alpha \\ 0 & 0 & e^{-\alpha T} \end{bmatrix} \quad (9)$$

The choice of α defines various manoeuvres i.e. it determines how long the manoeuvre last. For example, for lazy turns, $\tau_m \approx 60$ s and for evasive turns $\tau_m \approx 10 - 20$ s as given in [2]. The distribution for

acceleration is modelled as *ternary uniform mixture* (Fig. 1).

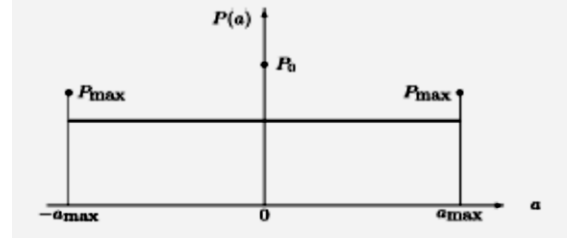


Fig.1: ternary uniform mixture pdf

The target moves with no acceleration with probability P_0 , accelerate or decelerate at a maximum acceleration a_{max} with a probability P_{max} , least accelerate or decelerate at a uniform rate distributed over $(-a_{max}, a_{max})$. Thus the variance of acceleration, σ^2 comes out as

$$\sigma^2 = \frac{a_{max}^2}{3} (1 + 4P_{max} - P_0) \quad (10)$$

As τ_m increases (i.e. αT decreases) The Singer model reduces to CA model and as τ_m decreases (i.e. αT increases) the model reduce to CV model. Hence for a choice of $0 < \alpha T < \infty$, The Singer model corresponds to a motion sliding in between nearly CV and nearly CA models. Hence it has a far wider coverage than CA and CV models.

Horizontal constant Turn model (HCT):

This model models a turn motion in horizontal plane as a 2D constant turn along with the height modelled as a CV motion with appropriate variance.

$$x_{k+1} = \text{diag}(F_\omega, F_{cv}) x_k + w_k^\omega \quad (11)$$

$$F_\omega = \begin{bmatrix} 1 & \frac{\sin \omega T}{\omega} & 0 & 0 & \frac{\cos \omega T - 1}{\omega} & 0 \\ 0 & \cos \omega T & 0 & 0 & -\sin \omega T & 0 \\ 0 & 0 & 0 & 0 & -\omega & 0 \\ 0 & \frac{1 - \cos \omega T}{\omega} & 0 & 1 & \frac{\sin \omega T}{\omega} & 0 \\ 0 & \sin \omega T & 0 & 0 & \cos \omega T & 0 \\ 0 & \omega & 0 & 0 & 0 & 0 \end{bmatrix} \quad (12)$$

$$F_{cv} = \begin{bmatrix} 1 & T & 0 \\ 0 & 1 & 0 \\ 0 & 0 & 0 \end{bmatrix} \quad (13)$$

w_k^ω is white noise sequence with covariance

$$Q_\omega = \text{diag}(S_x Q, S_y Q, S_z Q_{cv})$$

$$Q = \begin{bmatrix} \frac{T^5}{20} & \frac{T^4}{8} & \frac{T^3}{6} \\ \frac{T^4}{8} & \frac{T^3}{3} & \frac{T^2}{2} \\ \frac{T^3}{6} & \frac{T^2}{2} & T \\ \frac{T^4}{4} & \frac{T^3}{2} & \frac{T^2}{2} \\ \frac{T^3}{2} & \frac{T^2}{2} & T \\ \frac{T^2}{2} & T & 1 \end{bmatrix}$$

Where the turn rate ω is computed as

$$\omega = \frac{\dot{x}\dot{y} - \dot{y}\dot{x}}{\sqrt{\dot{x}^2 + \dot{y}^2}} \quad (14)$$

3D Constant Turn model (3DCT) :

This model models a turn motion in 3D space at a constant turn rate, Ω and a constant speed, where $\Omega = \|\Omega\|$; where $\Omega = [\omega_x, \omega_y, \omega_z]$ is the angular velocity vector.

Constant speed motion (i.e. $\dot{v} = 0$) corresponds to $\mathbf{a} \cdot \mathbf{v} = 0$, where \mathbf{a} and \mathbf{v} are acceleration and velocity vectors respectively. From the kinematic relations in 3D rotation, constant speed can be equivalently represented as suggested in [1]

$$\mathbf{a} = \Omega \times \mathbf{v} \quad (15)$$

Further, under the assumption that $\Omega \cdot \mathbf{v} = 0$, the angular velocity, after some vector operations can be written as

$$\Omega = \frac{\mathbf{v} \times \mathbf{a}}{v^2} \quad (16)$$

Eqn(16) implies that $\Omega \perp \mathbf{a}$, and that \mathbf{v} and \mathbf{a} are coplanar to which Ω is orthogonal. Thus the motion is planar (plane defined by \mathbf{a} and \mathbf{v} called manoeuvre plane), but not necessarily horizontal, if Ω has a constant direction. Eqn(16) holds true even if $\dot{\Omega} \neq 0$ and if Ω has a constant direction.

A constant turn rate motion (i.e. $\dot{\Omega} = 0$) can be deduced by differentiating eqn (15)

$$\dot{\mathbf{a}} = \Omega \times \mathbf{a} = \Omega \times (\Omega \times \mathbf{v}) = (\Omega \cdot \mathbf{v})\Omega - (\Omega \cdot \Omega)\mathbf{v} = -\omega^2 \mathbf{v} \quad (17)$$

$$\text{Where } \omega = \frac{\|\mathbf{v} \times \mathbf{a}\|}{v^2} = \frac{\|\mathbf{v}\| \|\mathbf{a}\|}{v^2} = \frac{a}{v} \quad (18)$$

The continuous state space model can be written as

$$\dot{\mathbf{x}}(t) = \text{diag}(A(\omega), A(\omega), A(\omega))\mathbf{x}(t) + \text{diag}(B, B, B)\mathbf{w}(t) \quad (19)$$

$$A(\omega) = \begin{bmatrix} 0 & 1 & 0 \\ 0 & 0 & 1 \\ 0 & -\omega^2 & 0 \end{bmatrix}, B = \begin{bmatrix} 0 \\ 0 \\ 1 \end{bmatrix} \quad (20)$$

Where $\mathbf{w}(t)$ is a white noise sequence with power spectral density $[S_x \ S_y \ S_z]$

Its discrete equivalent model turns out as given in

$$\mathbf{x}_{k+1} = \text{diag}(F_{3DCT}(\omega), F_{3DCT}(\omega), F_{3DCT}(\omega))\mathbf{x}_k + \mathbf{w}_k \quad (20)$$

$$F_{3DCT}(\omega) = \begin{bmatrix} 1 & \frac{\sin(\omega T)}{\omega} & \frac{1 - \cos(\omega T)}{\omega^2} \\ 0 & \cos(\omega T) & \frac{\sin(\omega T)}{\omega} \\ 0 & -\omega \sin(\omega T) & \cos(\omega T) \end{bmatrix} \quad (21)$$

$$Q_w = \text{cov}(\mathbf{w}_k) = \text{diag}(S_x Q_{3DCT}(\omega), S_x Q_{3DCT}(\omega), S_x Q_{3DCT}(\omega)) \quad (22)$$

$$Q_{3DCT}(\omega) = \begin{bmatrix} \frac{6\omega T - 8\sin(\omega T) + \sin(2\omega T)}{4\omega^5} & \frac{2\sin^4(\omega T/2)}{\omega^4} & \frac{-2\omega T + 4\sin(\omega T) - \sin(2\omega T)}{4\omega^3} \\ \frac{2\sin^4(\omega T/2)}{\omega^4} & \frac{2\omega T - \sin(2\omega T)}{4\omega^3} & \frac{\sin^2(\omega T)}{2\omega^2} \\ \frac{-2\omega T + 4\sin(\omega T) - \sin(2\omega T)}{4\omega^3} & \frac{\sin^2(\omega T)}{2\omega^2} & \frac{2\omega T + \sin(2\omega T)}{4\omega} \end{bmatrix} \quad (22)$$

III. OVERVIEW OF IMM ALGORITHM

IMM Algorithm is a multiple motion model in which r different models interact with each other to give the estimate of a state of a target at each sampling time. One cycle of the algorithm is given in fig.2.

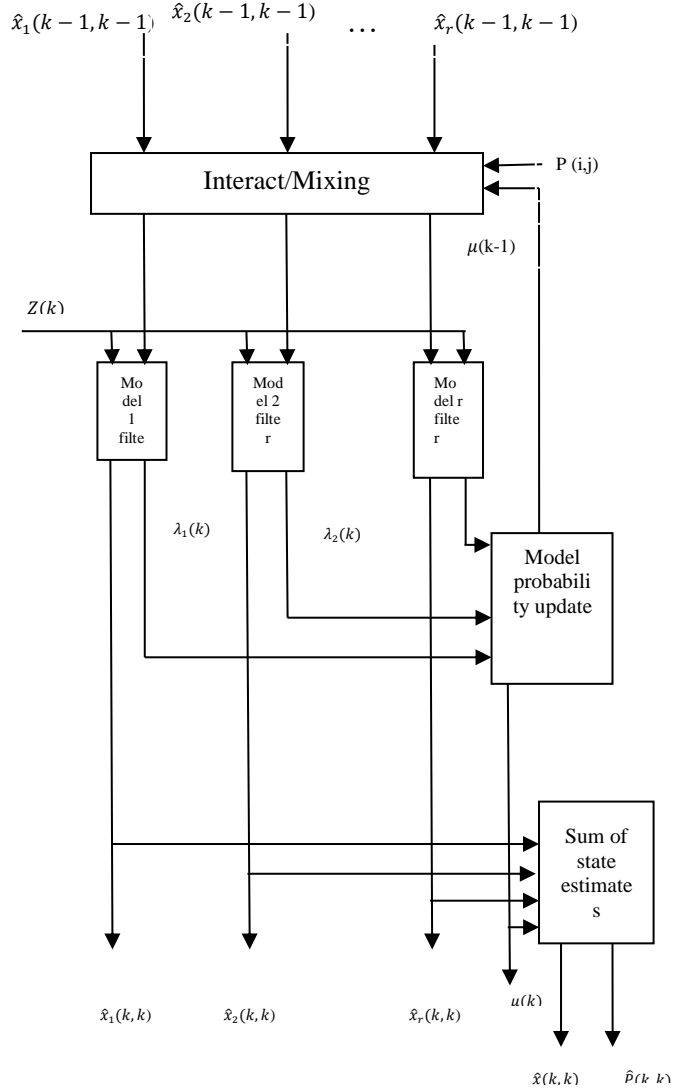


Figure 2: One cycle of IMM filter

Model switching probability $P(i, j)$ and model probability $\mu(k-1)$ forming mixed state estimates for each model. Subsequently, Filtering at each model based filter takes place based on the measurements available at the instant k . Likelihood of each filter estimate with the measurement, $\lambda_1(k), \lambda_2(k), \dots, \lambda_r(k)$, updates model probability $\mu(k)$ of each filter. The state estimate $\hat{\mathbf{x}}(k, k)$, and the Covariance $\hat{\mathbf{P}}(k, k)$ is computed based on the updated model probability $\mu(k)$.

IMM1 comprises of 5 singer models with α suited to different motion. The choice of α for the models is given in table.1 as suggested in [14]. IMM2 comprises of CA, HCT and 3DCT models. The turn rate, ω for HCT and 3DCT are computed as in (14) and (17) respectively.

IV. SIMULATION AND RESULTS

We have simulated few sophisticated test trajectories to compare IMM comprising of Singer models with different α (IMM1) and an IMM (IMM2) comprising of CA, HCT and 3DCT models. The different α values used for simulations are shown in Table.1. The sampling interval T is 0.5 s. In first scenario the target first rises up in CV motion for 60 scans then takes HCT turn at $\omega = 3 \text{ deg/s}$ for 130 scans and moves with CV for next 60 scans. In second scenario the target first rises up in CV motion for 60 scans, then takes HCT turn at $\omega = 3 \text{ deg/s}$ for 60 scans, then moves with a constant speed for next 10 scans, then takes a 3DCT turn with angular velocity Ω , such that $\Omega \perp v$ for another 60 scans, then moves in CV motion for the next 20 scans and finally takes a HCT turn at $\omega = 4 \text{ deg/s}$ for 40 scans. The trajectories are shown in Fig. 3 and Fig. 4.

Set	α_x	α_y	α_z
1	1/60	1/60	1/60
2	1/60	1/60	1
2	1	1	1/60
4	1	1	1
5	1/10	1/10	1/40

Table 1. Parameter for Singer models

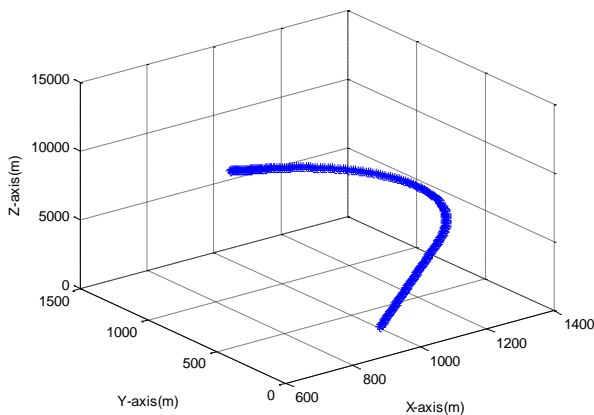


Figure 4: Simulated trajectory scenario 1

The test results are plotted after 100 Monte Carlo runs. It is assumed that we get only position measurements from the RADAR, corrupted with white noise with standard deviations $\sigma_r = 1 \text{ m}$, $\sigma_\theta = 0.1 \text{ deg}$, $\sigma_\phi = 0.1 \text{ deg}$ in range, azimuth and elevation respectively. The measurements are converted to unbiased Cartesian coordinates as suggested in [13]. Positional errors of IMM with CV, CA and are plotted and compared with IMM with singer model for both scenarios. For 2D turn case the Positional error between radar measurements and true value (\mathcal{E}_{PM}) is always less than the positional errors between true measurement and IMM ($\mathcal{E}_{PSINGER}$) with singer model and positional error between true measurement and IMM (\mathcal{E}_{PIMM2}) with CV,

HCT model and 3DCT model. The error graphs are given below.

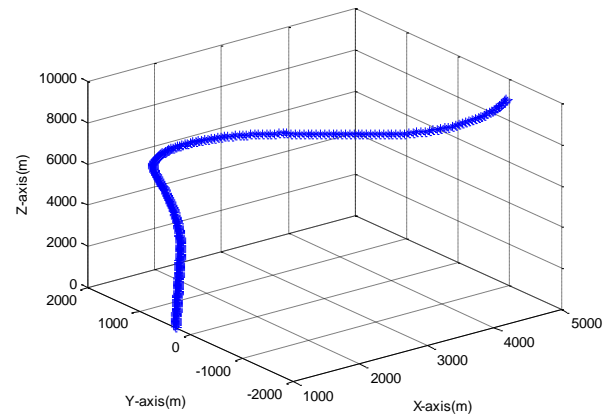


Figure 4: Simulated trajectory for scenario 2

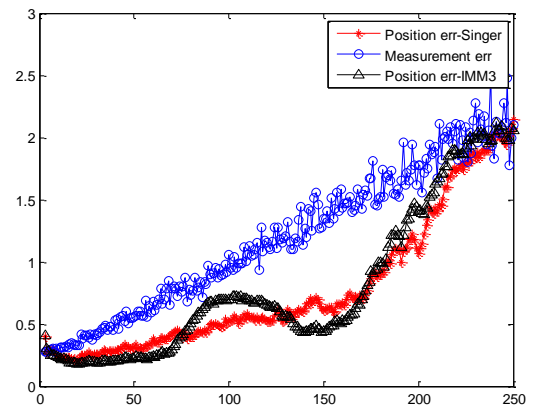


Figure 7 : Comparison of positional errors between Singer model and IMM (CV,HCT and 3DCT) for scenario 1

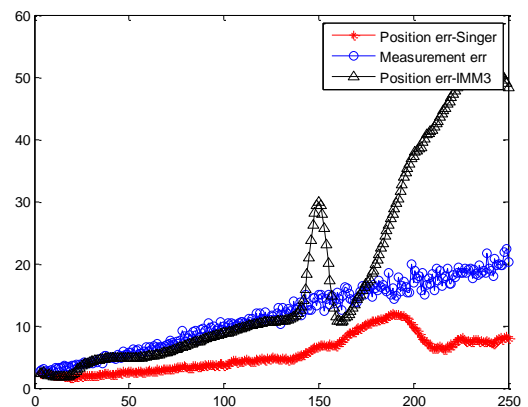


Figure 8: Comparison of positional errors between Singer and IMM (CV,HCT and 3DCT) for scenario 2

Total 100 monte carlo runs are used for calculating the root mean errors. Here M is the number of Monte carlo runs $M = 1, 2, \dots, 100$.

$$\mathcal{E}_{PM} = \sqrt{\frac{\sum_{i=1}^M \mathcal{E}_r^2(i)}{M}} \quad \text{where } \mathcal{E}_r = \text{positional error}$$

for each scan between radar measurements and true values, \mathcal{E}_{PM} is the root mean square error (RMS) for 100 Monte Carlo runs.

$$\mathcal{E}_{PIMM2} = \sqrt{\frac{\sum_{i=1}^M \mathcal{E}_{rimm2}^2(i)}{M}} \quad \text{where } \mathcal{E}_{rimm2} =$$

positional error for each scan between IMM2 estimated values and true values, \mathcal{E}_{PIMM2} is the RMS error for 100 Monte Carlo runs.

$$\mathcal{E}_{PSINGER} = \sqrt{\frac{\sum_{i=1}^M \mathcal{E}_{rsinger}^2(i)}{M}} \quad \text{where } \mathcal{E}_{rsinger} =$$

positional error for each scan between IMM with singer model estimated values and true values, $\mathcal{E}_{PSINGER}$ is the RMS error for 100 Monte Carlo runs.

The RMS errors are plotted and are shown in Fig. 7 and Fig. 8. it is observed that for horizontal turns both singer and IMM2 are reducing the error compared to measurement error, where are for 3D turns singer is performing well compared to IMM2. Clearly the error graphs will depicts the same.

V. CONCLUSION

In this paper it is attempted to study the performance of the IMM filter with different models for horizontal (2D) turns and a combination of Horizontal and Vertical (3D) turns. We have showed that the estimated trajectories for horizontal turns for IMM (IMM2) with CV, CA and 3DCT model and IMM with singer models are performing well and the error graphs plotted will show that the RMS errors are less than the RMS error of measurements. For 3D turns IMM with singer model is outperforming the IMM2 filter and the Monte Carlo simulation results confirm the same.

ACKNOWLEDGEMENTS

The authors would like to thank Mr. Mahesh.V Chief Scientist and Management of Bharat Electronics Limited for encouragement and support to write this paper. Also authors express sincere thanks to C.R. Patil, Senior Member Research Staff, BEL for their helpful contribution in this research work.

REFERENCES

- [1] Li, X. R., and Jilkov, V. P. (2000) "A survey of maneuvering target tracking: Dynamic models", In *Proceedings of the 2000 SPIE Conference on Signal and Data Processing of Small Targets*, Vol. 4048, Orlando, FL, Apr. 2000, 212–236.
- [2] Singer, R. A. (1970) "Estimating optimal tracking filter performance for manned maneuvering targets", *Transactions on Aerospace and Electronic Systems*, **AES-6** (July 1970), 473–483.

- [3] Zhou, H., and Kumar, K. S. P. (1984) "A current statistical model and adaptive algorithm for estimating maneuvering targets", *AIAA Journal of Guidance*, **7**, 5 (Sept.–Oct. 1984), 596–602.
- [4] Li, X. R., and Bar-Shalom, Y. (1993) "Design of an interacting multiple model algorithm for air traffic control tracking", *IEEE Transactions on Control Systems Technology*, **1**, 3 (Sept. 1993), 186–194; special issue on air traffic control
- [5] Blom, H. A. P., Hogendoorn, R. A., and van Doorn, B. A. (1992) "Design of a multisensor tracking system for advanced air traffic control", In Y. Bar-Shalom (Ed.), *Multitarget-Multisensor Tracking: Applications and Advances*, Vol. II, Norwood, MA: Artech House, 1992, ch. 2.
- [6] Bryan, R. S. (1980) "Cooperative estimation of targets by multiple aircraft", M.S. thesis, Air Force Institute of Technology, Wright-Patterson AFB, Ohio, June, 1980.
- [7] Maybeck, P. S., Worsley, W. H., and Flynn, P. M. (1982) Investigation of constant turn-rate dynamics for airborne vehicle tracking. In *Proceedings of the National Aerospace and Electronics Conference (NAECON)*, 1982, 896–903.
- [8] Zhan, R., Wan, J.: "Passive maneuvering target tracking using 3D constant-turn model", *IEEE Conf. on Radar*, 2006, Verona, USA, April 2006, pp. 404
- [9] Berg, R. F. (1983) "Estimation and prediction for maneuvering target trajectories", *IEEE Transactions on Automatic Control*, **AC-28** (Mar.1983), 294–304.
- [10] Blom, H., Bar-Shalom, Y.: "An efficient filter for abruptly changing systems", *Proc.23rd IEEE Conf. on Decision and Control*, Las Vegas, USA, December 1984, pp. 656–658.
- [11] Watson, G., Blair, W.: "IMM algorithm for tracking targets that maneuver through coordinated turns", *Fourth Conf. on the Signal and Data Processing of Small Targets*, Orlando FL, USA, August 1992, pp. 236–247
- [12] Yang, N., Tian, W., Jin, Z.: 'An interacting multiple model particle filter for maneuvering target location', *Meas. Sci. Technol.*, 2006, **17**, (6), pp. 1307–13
- [13] Mo Longbin, SongXiaoquan, "Unbiased Converted Measurements for Tracking" *IEEE Transactions on AeroSpace and Electronic Systems*, Correspondence VOL. 34 NO 3 JULY 1988, pp 1023-1027.
- [14] Lihua Zhu, Xianghong Cheng, "High manoeuvre target tracking in coordinated turns", *Key Laboratory of Micro Inertial Instrument and Advanced Navigation*, Southeast University, ISSN 1751-8784, 2015, April



Fahad A. M. obtained B.Tech in Electronics and Communications from Cochin University of Science and Technology and Masters in communications systems from NIT Surat. His research activities include Radar Signal Processing and Estimation and Motion modeling.



G Sampath Kumar obtained his B.Tech degree in Electronics and communication Engineering from Sree Vidyanikethan Engineering college and Masters in Communications from IIT Delhi, Delhi and is currently working as memeber research staff at Central Research Laboratory, BEL. His research activities include Radar signal processing, Multi target tracking, and Sensor Data Fusion.



Dr. VIJI PAUL P. is working as Member Senior Research Staff at Central Research Laboratory, BEL. His research activities include Radar signal processing, Multi target tracking, and Sensor Data Fusion. He obtained PhD degree in Electrical Engineering from IIT Bombay.



L Ramakrishnan obtained B.Tech (Electronics Engg) MIT, Anna University & ME (ECE) OU. Starting his career at HAL, worked in various projects including Air borne Transponders, Airborne radar for modern Indian fighter aircrafts, Air Route Surveillance Radar, Radio Proximity fuses etc. His area of professional interest includes Design and Development of front ends for Radar, Wireless & Communications Systems. He is currently serving as Principal Scientist & Group Head at Central Research Laboratory, BEL. He presently is involved in the design and development of embedded computing products & signal processing sub systems for radar applications. He has over fifteen reputed publications to his credit. As part of team, he has been bestowed with Raksha Mantri's award under Innovation Category and BEL R&D Excellence Awards. He is Member (IEEE) and certified PMP.